National Aeronautics and Space Administration

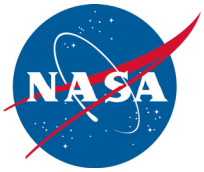

SiC *vs.* Si for High Radiation Environments

Richard D. Harris
Jet Propulsion Laboratory
Pasadena, California

Jet Propulsion Laboratory
California Institute of Technology
Pasadena, California

JPL Publication 08-6 2/08

National Aeronautics and Space Administration

SiC *vs.* Si for High Radiation Environments

NASA Electronic Parts and Packaging (NEPP) Program
Office of Safety and Mission Assurance

Richard D. Harris
Jet Propulsion Laboratory
Pasadena, California

NASA WBS: 939904.01.11.30
JPL Project Number: 102197
Task Number: 3.32.7

Jet Propulsion Laboratory
4800 Oak Grove Drive
Pasadena, CA 91109

http://nepp.nasa.gov

This research was carried out at the Jet Propulsion Laboratory, California Institute of Technology, and was sponsored by the National Aeronautics and Space Administration Electronic Parts and Packaging (NEPP) Program.

SiC vs. Si for High Radiation Environments

Richard D. Harris

NEPP Program
Office of Safety & Mission Assurance
WBS 939904.01.11.30 under TASK ORDER NMO7-10824
Project Number: 102197
Task Number: 3.32.7

1/15/2008

PI: Richard D. Harris

Abstract—Commercial silicon carbide and silicon Schottky barrier power diodes have been subjected to 203 MeV proton irradiation and the effects of the resultant displacement damage on the I-V characteristics have been observed. Changes in forward bias I-V characteristics are reported for fluences up to 4×10^{14} p/cm^2. For devices of both material types, the series resistance is observed to increase as the fluence increases. The changes in series resistance result from changes in the free carrier concentration due to carrier removal by the defects produced. A simple model is presented that allows calculation of the series resistance of the device and then relates the carrier removal rate to the changes in series resistance. Using this model to calculate the carrier removal rate in both materials reveals that the carrier removal rate in silicon is less than that in silicon carbide, indicating that silicon is the more radiation tolerant material.

Table of Contents

SECTIONS

TABLES

FIGURES

APPENDICES

1.0 INTRODUCTION

NASA has considered future missions that could use nuclear reactors to provide more power for propulsion, scientific instruments, etc. than is available with current systems. Such a reactor system would require the use of components with much higher power ratings than those presently used. In addition, there are several missions being considered that would expose the electronics to very high radiation environments (e.g., missions to Jupiter, Jupiter's moon Europa, and certain high fluence Earth orbits). These future missions, therefore, provide a double challenge; first, to evaluate and qualify a new class of higher power components, and second, to extend the radiation tolerance of power devices to much higher fluences.

In previous papers, the effects of proton irradiation on silicon carbide Schottky barrier diodes [1] and silicon Schottky barrier diodes [2] were discussed. The results presented in these papers indicate that Schottky barrier diodes from both materials are inherently hard to displacement damage induced by high-energy proton irradiation. Furthermore, those results show that there is no change in the characteristics of the Schottky contact and that the only change observed in the forward voltage drop can be explained by changes in the series resistance. The change in series resistance can in turn be explained by changes in the free carrier concentration due to carrier removal caused by defects resulting from displacement damage. As a result, Schottky barrier diodes can serve as a good device for comparing the radiation response of the different materials as monitored through the carrier removal rate.

Previous papers have indicated that the radiation hardness of SiC is expected to be greater than that of Si [3]–[5]. In the present paper, Schottky barrier diodes are employed to make a direct comparison between the carrier removal rates of silicon and silicon carbide with irradiation occurring under identical beam conditions.

2.0 EXPERIMENTAL PROCEDURE

The parts used in this study include commercial 4H silicon carbide Schottky barrier diodes purchased from Cree, Inc. and silicon Schottky barrier diodes purchased from International Rectifier, Inc. (IR). The part numbers and their ratings are listed in Table I.

Devices were irradiated at the Indiana University Cyclotron Facility (IUCF) with 203 MeV protons. Dosimetry was provided by IUCF. In this study, devices were irradiated to total fluences between 2.0×10^{14} and 4.4×10^{14} p/cm^2. The average flux during irradiation varied between 1.5×10^{10} and 5×10^{10} p/cm^2/s. All irradiations in this study were carried out at room temperature.

All devices were unbiased while being irradiated. I-V characteristics were measured at various fluences during the irradiation. The proton beam was interrupted while electrical measurements were made to avoid interference from currents generated by the proton beam. In all cases, electrical measurements were taken immediately after the proton beam was stopped and all measurements were taken at room temperature.

I-V measurements were made with two different instruments: a Tektronix 371B High Power Curve Tracer was used to take data in forward bias at higher currents, while a Keithley 4200SCS Semiconductor Characterization System was used to take data at lower currents in forward bias. Details of the irradiation setup are provided in the previous papers [1], [2].

TABLE I
INFORMATION ON PARTS USED IN THIS STUDY

Supplier	Material	Part Number	Voltage Rating	Current Rating
Cree, Inc.	SiC	CSD10120A	1200 V	10 A
Cree, Inc.	SiC	CSD10120D	1200 V	5 A
Cree, Inc.	SiC	CSD10060A	600 V	10 A
Cree, Inc.	SiC	CSD04060A	600 V	4 A
Cree, Inc.	SiC	CSD10030A	300 V	10 A
IR	Si	60CTQ150	150 V	30 A
IR	Si	40CTQ150	150 V	20 A
IR	Si	10CTQ150	150 V	5 A
IR	Si	113CNQ100A	100 V	55 A
IR	Si	43CTQ100	100 V	20 A
IR	Si	48CTQ060	60 V	20 A

For the data analysis, it is necessary to determine the free carrier concentrations of the diodes used in the irradiations. Unfortunately, the irradiations were performed prior to the data analysis and the free carrier concentrations were not determined on the individual diodes prior to their being irradiated. Instead, diodes from the same lot and date code as the irradiated diodes were subjected to C-V measurements. Between eight and ten of each diode part number were measured in order to get an estimate of the variation within the lot.

Measurements were performed with an HP 4280A 1 MHz capacitance meter. The capacitance was measured for reverse biases extending from 0 V to 40 V. Plots of $1/C^2$ *vs.* V were made and the slopes determined (see Appendices A and B for the plots). The free carrier concentration was determined from the relationship [6]:

$$1/C^2 = 2(V_{bi} + V)/q\varepsilon\varepsilon_0 N_D A^2, \quad (1)$$

where C is the capacitance, V_{bi} is the built-in potential, V is the applied reverse bias, q is the electronic charge, ε is the dielectric constant of the material, ε_0 is the permittivity of free space, N_D is the free carrier concentration, and A is the diode area. The diode areas were determined by removing the plastic packaging on the part and measuring the active area under a microscope. Details of the $1/C^2$ *vs.* V results are described in the Appendices.

3.0 EXPERIMENTAL RESULTS

Representative I-V characteristics are shown in Fig. 1 for a typical 1200V/10A SiC Schottky barrier diode from Cree, Inc. (part number CSD10120A) and in Fig. 2 for a typical 60V/20A Si Schottky barrier diode from IR (part number 48CTQ060) for selected fluences. The number of fluences shown in these figures is less than the number measured so as minimize the clutter in the figures. In these figures, the closed symbols represent data taken with the Keithley 4200SCS while the open symbols represent data taken with the Tektronix 371B.

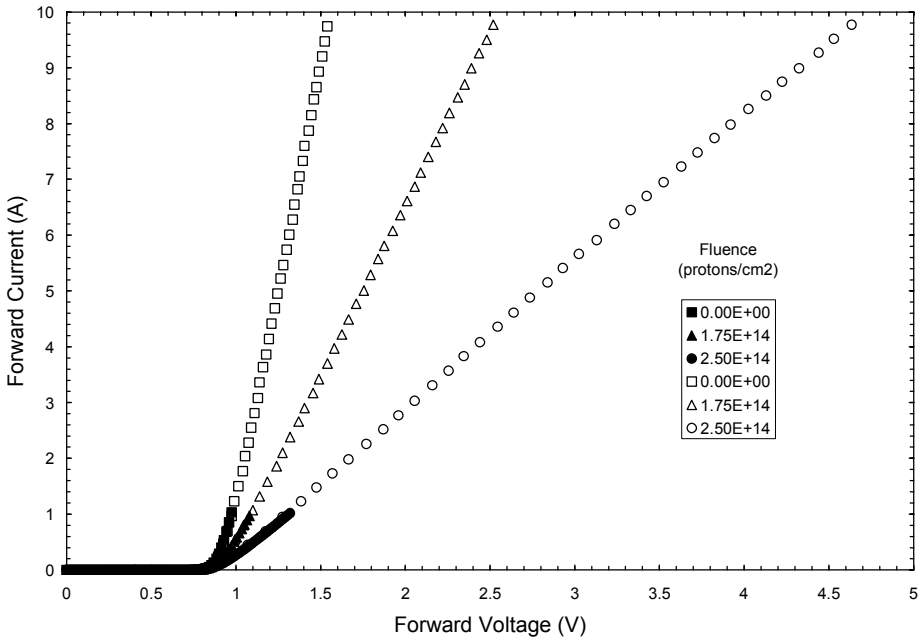

Fig. 1 Forward bias I-V characteristics *vs.* 203 MeV proton fluence for selected fluences for 1200V/10A SiC Schottky barrier diode. (Figure is from [1].)

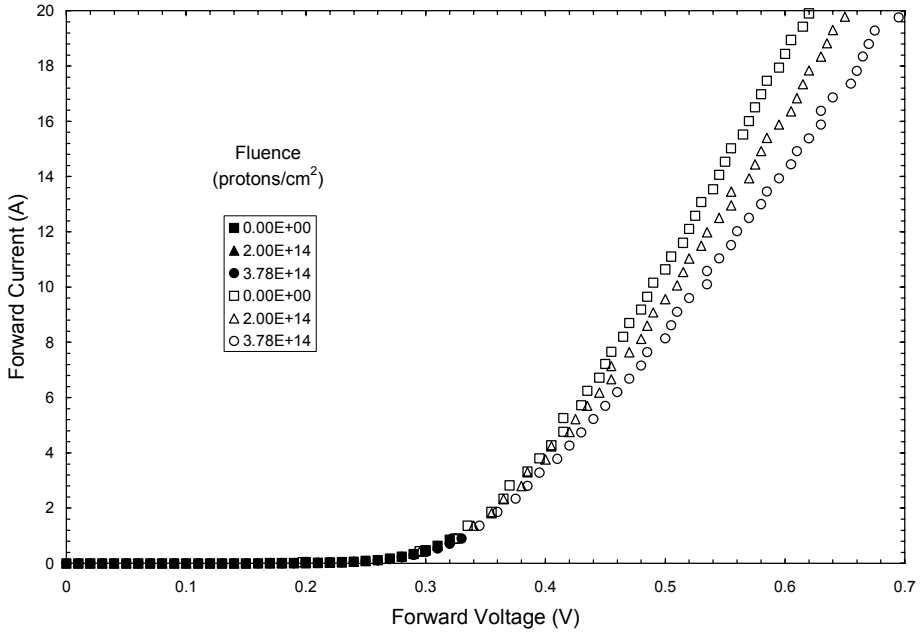

Fig. 2 Forward bias I-V characteristics *vs.* 203 MeV proton fluence for selected fluences for 60V/20A Si Schottky barrier diode. (Figure is from [2].)

As the proton fluence increases, the forward bias voltage increases, as seen in Figs. 1 and 2. This is a typical result for radiation damage in semiconductors, although for these Schottky barrier devices there is little change observed until fluences are well into the 10^{14} p/cm^2 range for both materials. These are very large fluences, indicating the exceptional robustness of both the Si and the SiC Schottky barrier diodes to displacement damage. Similar results to those shown in Figs. 1 and 2 are seen for all Schottky barrier diodes studied.

4.0 DISCUSSION AND ANALYSIS

In this paper, the goal is to compare the results of the Schottky barrier diodes fabricated from the different materials, SiC and Si, that were irradiated in the previous papers [1], [2]. One way to directly compare the radiation resistance of the two materials is by looking at the fluence at which substantial changes in the forward characteristic are observed to begin. This is most easily done by plotting the forward voltage at a fixed forward current as a function of the proton fluence.

The result of this procedure is shown in Fig. 3 for two SiC samples and two Si samples where the forward current for all samples is 1 A. The SiC samples depicted are CSD10120A (1200V/10A) and CSD10030A (300V/10A) while the Si samples are 40CTQ150 (150V/20A) and 48CTQ060 (60V/20A). Also shown in the figure, with open symbols, are two Si p-n diodes for comparison [7]. These Si p-n diodes are from IR p/n IRKJ91/16A (1600V/100A) and Semikron p/n SKN141F12 (1200V/168A).

The first thing that is immediately apparent from Fig. 3 is the large difference in the onset of forward voltage shifts between the Si p-n diodes and all of the Schottky diodes. The onset of forward voltage increase starts in the low 10^{13} p/cm^2 range for the Si p-n diodes while all of the

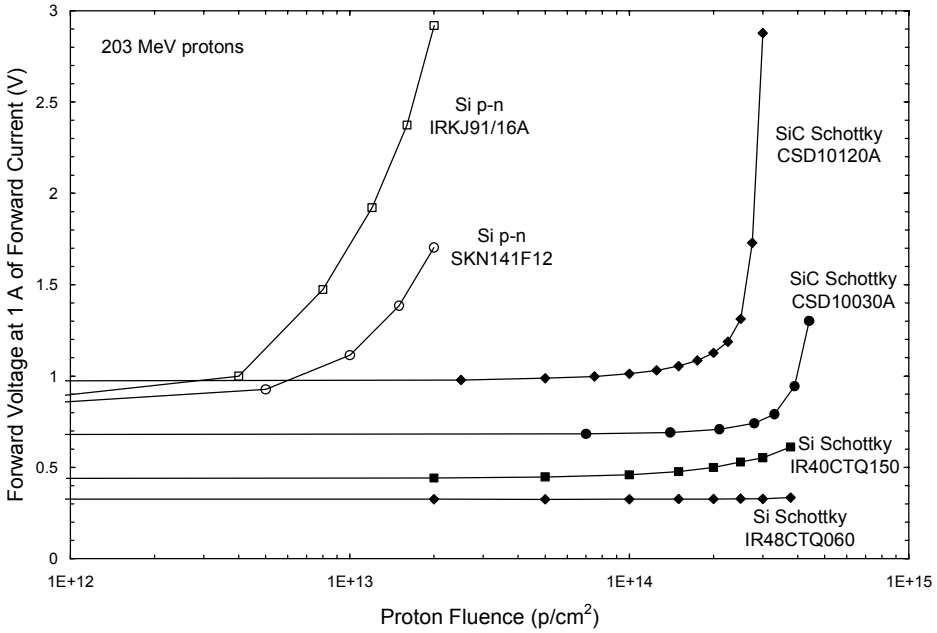

Fig. 3 Comparison of forward voltage changes as a function of proton fluence for several Schottky barrier diodes and p-n diodes.

Schottky diodes remain unchanged well into the 10^{14} p/cm^2 range. This observation demonstrates that the Schottky diode structure is clearly a much more robust structure than the p-n structure; undoubtedly due to the fact that the p-n diodes are minority carrier devices, where both minority carrier lifetime degradation and carrier removal contribute to the damage, and the Schottky diodes are majority carrier devices, where only carrier removal contributes to the damage.

For the SiC Schottky diodes, the onset of forward voltage increases begins at fluences between 2×10^{14} and 4×10^{14} p/cm^2. For the Si Schottky diodes, there is no significant increase in the forward voltage up to the limit of the proton fluence explored in this experiment, 3.8×10^{14} p/cm^2. This observation suggests that the Si Schottky diodes are even more robust that the SiC Schottky diodes.

It is possible to quantify this observation by calculating the carrier removal rates from these results. In the previous papers [1], [2], a procedure was described for determining the carrier removal rate from the radiation-induced forward voltage increases in a Schottky barrier diode. That procedure is reviewed here.

The measured forward I-V curve of the diode can be fit to the ideal diode equation:

$$I = I_S\{\exp[q(V - I\cdot R_S)/nkT] - 1\}, \quad (2)$$

where I is the measured current, I_S is the saturation current, q is the electronic charge, V is the applied voltage, R_S is the series resistance, n is the diode ideality factor, k is Boltzmann's constant, and T is the temperature.

The fitting is most easily accomplished in two steps. First, the low injection region is fit to obtain the saturation current and the ideality factor. Then, the high injection region is fit to give the series resistance. The forward bias data for all measured Schottky barrier diodes fit the ideal diode equation (2) very well. Examples of the fit are shown in Figs. 4 and 5.

Fig. 4 shows a fit of the ideal diode equation to the forward bias low injection region of the data of a Si 60V/20A Schottky diode (48CTQ060) following irradiation with 3.8×10^{14} p/cm^2 and using the parameters shown in the figure caption. The plot is a semilog plot to best display the low injection region. Fig. 5 shows a fit of the ideal diode equation to the forward bias high injection region of the same data. The plot is a linear plot as that best displays the high injection region.

As was discussed previously [1], [2], there are no substantial changes in the low injection region as the irradiation proceeds, indicating that there is no degradation of the Schottky contact. The parameter that does show substantial changes is the series resistance. It is the changes in this parameter that give rise to the changes observed in Figs. 1 and 2.

Furthermore, it was concluded that these changes in the series resistance can be explained entirely by carrier removal caused by the production of defects due to displacement damage. The series resistance is inversely proportional to the free carrier concentration [6]:

$$R_S = K / N_D, \quad (3)$$

where K is a constant that depends on the relationship between free carrier concentration and resistivity and on the diode geometry, and N_D is the free carrier concentration in the material.

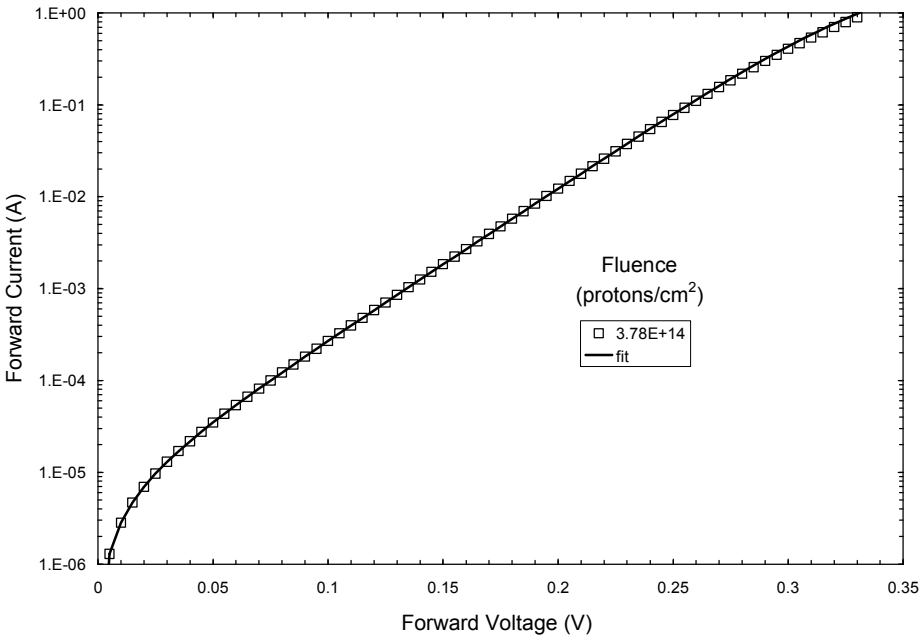

Fig. 4 Fit of forward bias low injection region of 60V/20A Si Schottky diode (48CTQ060) irradiated with 3.8×10^{14} p/cm^2 to the ideal diode equation with parameters $I_S = 6.10 \times 10^{-6}$ A, $n = 1.034$, and $R_S = 0.0151\ \Omega$. (Figure is from [2].)

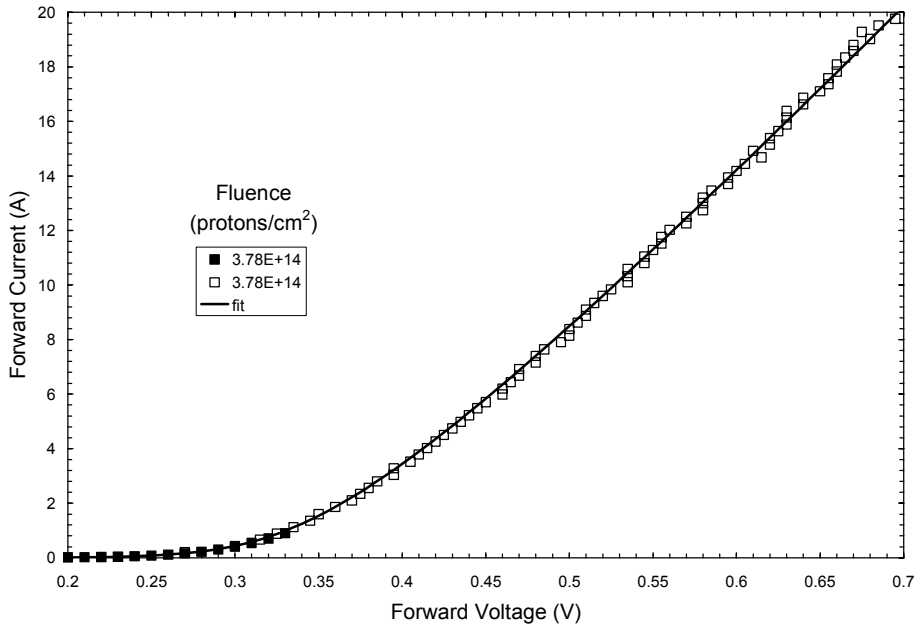

Fig. 5 Fit of forward bias high injection region of 60V/20A Si Schottky diode (48CTQ060) irradiated with 3.8×10^{14} p/cm^2 to the ideal diode equation with parameters $I_S = 6.10 \times 10^{-6}$ A, $n = 1.034$, and $R_S = 0.0151\ \Omega$. (Figure is from [2].)

The displacement damage causes carrier removal that decreases the free carrier concentration per:

$$N_D = N_{D0} - R_{CR} \cdot \Phi \,, \tag{4}$$

where N_D is the free carrier density, N_{D0} is the pre-irradiation free carrier density, R_{CR} is the carrier removal rate, and Φ is the proton fluence. Combining (3) and (4), the relationship between series resistance and irradiation fluence is given by:

$$1/R_S = \left(N_{D0} - R_{CR} \cdot \Phi\right)/K \,. \tag{5}$$

As a result, a plot of $1/R_S$ *vs.* Φ is a straight line where the intercept is related to the initial free carrier concentration and the slope is related to the carrier removal rate.

Table II shows the initial free carrier concentration as determined from the C-V measurements and (1). Plots of $1/C^2$ *vs.* V are shown for the different part numbers in the appendices. Also shown in the table are the areas determined by optical inspection of the die.

Fig. 6 shows the plot of $1/R_S$ *vs.* Φ for all the SiC Schottky diodes and Fig. 7 shows the plot for all the Si Schottky diodes studied. For each data set, a very linear dependence is observed, as predicted by (5). It is actually quite remarkable that the behavior is explained so well by such a simple model.

The slopes of some of the lines in Figs. 6 and 7 appear to be very different. This is anticipated from (5), where the slope is given as R_{CR}/K. The constant K contains device geometry terms, specifically the diode active area and the thickness of the active area, which are expected to be very different for the different device ratings. Therefore, it is concluded that the origin of the apparent slope differences in Figs. 6 and 7, for devices of the same voltage rating and therefore the same initial free carrier concentration, is entirely device geometry related.

In the previous papers [1], [2], the initial free carrier concentration was not known and so the carrier removal rate could not be calculated. C-V measurements have now been performed on diodes from the same lot as the irradiated parts in order to determine the free carrier

TABLE II
PART PARAMETERS DETERMINED FROM C-V MEASUREMENTS

Part Number	Area (cm^2)	Initial Free Carrier Concentration(cm^{-3})
CSD10120A	0.0635	3.87E+15
CSD10120D	0.0489	2.27E+15
CSD10060A	0.0449	5.91E+15
CSD04060A	0.0184	5.00E+15
CSD10030A	0.0232	8.85E+15
60CTQ150	0.157	8.77E+14
40CTQ150	0.113	9.09E+14
10CTQ150	0.0329	9.39E+14
113CNQ100A	0.2875	2.10E+15
43CTQ100	0.112	1.99E+15
48CTQ060	0.111	3.96E+15

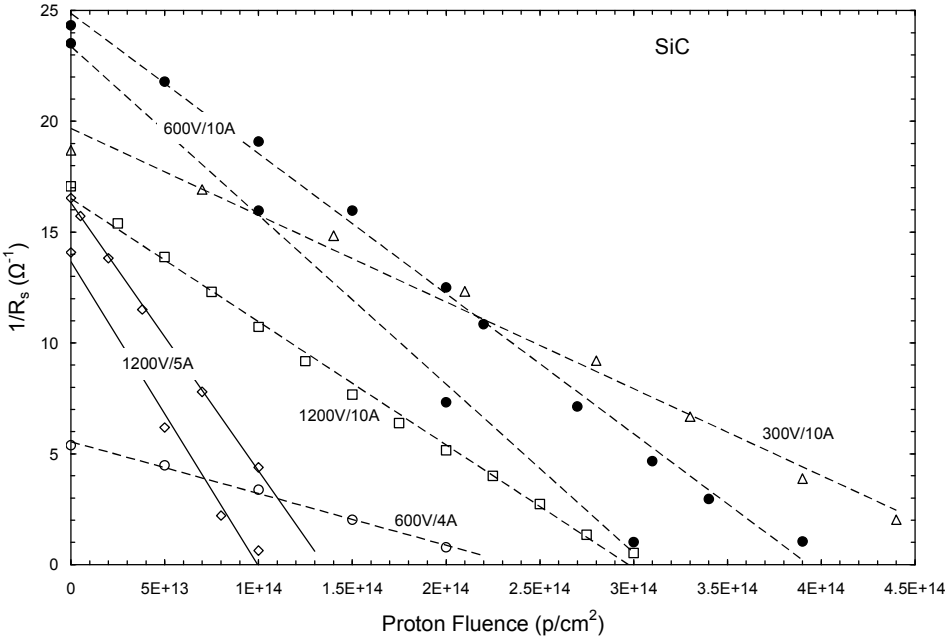

Fig. 6 Plot of the inverse of the series resistance *vs*. proton fluence for the SiC Schottky diodes. The lines are the fits used to determine the parameters in (5).

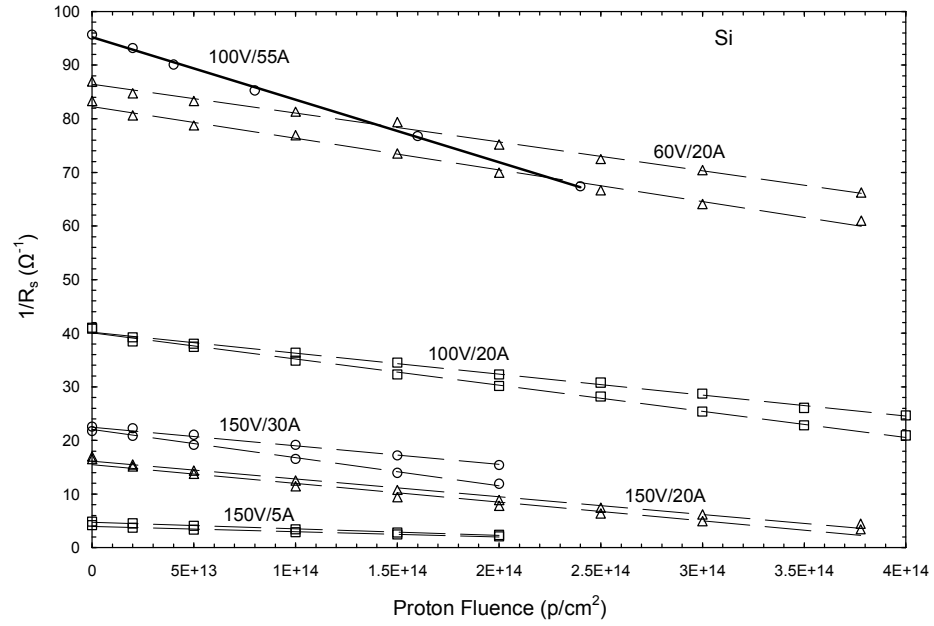

Fig. 7 Plot of the inverse of the series resistance *vs*. proton fluence for the Si Schottky diodes. The lines are the fits used to determine the parameters in (5).

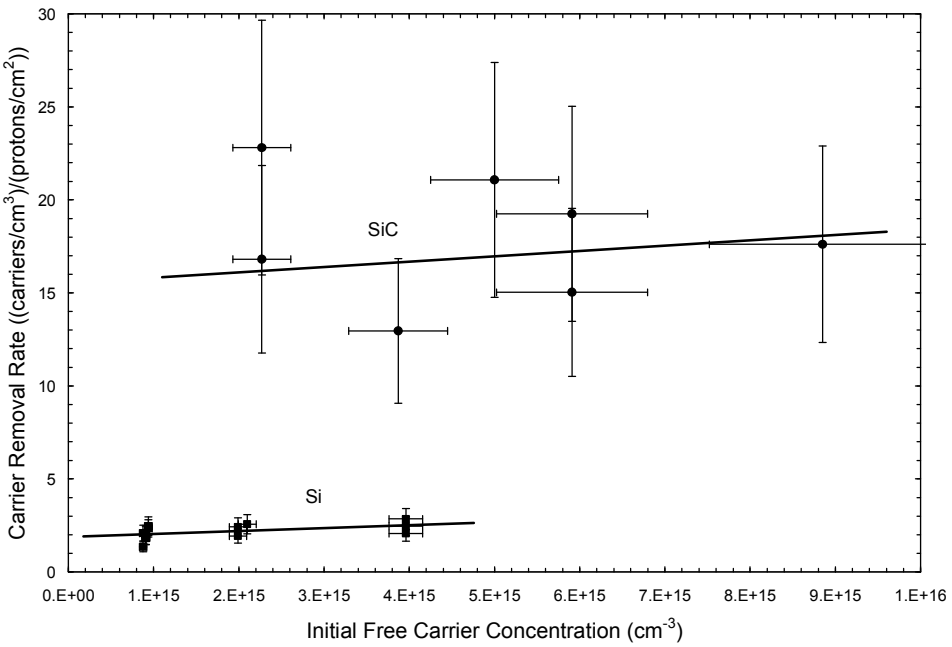

Fig. 8 Plot of carrier removal rate *vs.* initial free carrier concentration for SiC and Si. The lines are merely meant to guide the eye.

concentration of the diodes prior to irradiation. As such, it is now possible to calculate the carrier removal rates for all the diodes studied.

The lines in Figs. 6 and 7 are the fits used for each data set to obtain the parameters in (5). Once the y-intercept and the slope of the fits are obtained, the carrier removal rate is:

$$R_{CR} = \text{slope} \cdot N_{D0} / \text{y} - \text{intercept}, \qquad (6)$$

by using (5).

The carrier removal rates so obtained are plotted in Fig. 8 against the measured free carrier concentration for both materials. Plotting against the initial free carrier concentration is a way of comparing the results in the two different materials. The carrier removal rates in SiC are higher than those in Si for comparable free carrier concentrations by approximately a factor of eight. The lines on the plot are merely meant to guide the eye. They are drawn with a positive slope as it is expected that the carrier removal rate will be higher for higher doping levels. The error bars on the data shown here are too large to make any statement on the change of carrier removal rate with doping density.

Fig. 8 shows error bars that have been estimated from the following factors. The error in the free carrier concentration comes from the measured scatter in the C-V measurements. This scatter results from the part-to-part variation within the production lot. (The plots are shown in the appendices.) This error would be considerably less if the parts that were going to be irradiated had been individually measured prior to irradiation. The error in R_{CR} comes from two factors: 1) the free carrier concentration which appears in (6), and 2) the error in beam dosimetry. The data shown here were taken in three completely separate trips to IUCF; two to irradiate SiC parts and one to irradiate the Si parts. As a result, there is the absolute error in

dosimetry along with some relative error in dosimetry that would have been minimized if all the irradiations had taken place in one trip.

The error in the SiC parts is quite a bit more than that in the Si parts due to the much larger variation in the C-V results for the SiC parts. This is reasonable as Si processing is expected to be better controlled than SiC processing. In any case, even with the large error bars, the carrier removal rates in SiC are much larger than those in Si.

The data in Fig. 6 were analyzed using (6) as if there was no change in R_{CR} with irradiation. However, the removal of carriers lowers the free carrier density; as mentioned above, it is expected that there is a variation of the carrier removal rate with doping density. This apparent discrepancy is explained by looking closely at the amount of carrier removal that occurs during the irradiation. The result is that the carrier removal is relatively small compared to the initial carrier density for most fluences; and so the carrier concentration is not changing in any appreciable way during the irradiation. This is true for all fluences but those which produced the lowest couple values of $1/R_S$, which possibly look like they are starting to turn upwards. This is expected, as at these fluences, the carrier removal may be becoming significant.

Another way to compare the two materials is to plot the carrier removal rate against supplier's voltage rating. Figs. 8 and 9 are closely related in that higher breakdown voltages are achieved with lower doping densities [6]. This comparison is relevant to a circuit designer who is picking parts based on ratings. Fig. 9 shows the carrier removal rates plotted against the supplier's voltage rating for the same devices shown in Fig. 8. Again, the considerable difference in the carrier removal rates for the two materials is readily apparent in the figure.

The larger carrier removal rate observed for SiC than for Si leads to the conclusion that Si is the more radiation-tolerant material. This conclusion is contrary to conventional wisdom that indicates that SiC should be more radiation tolerant than Si.

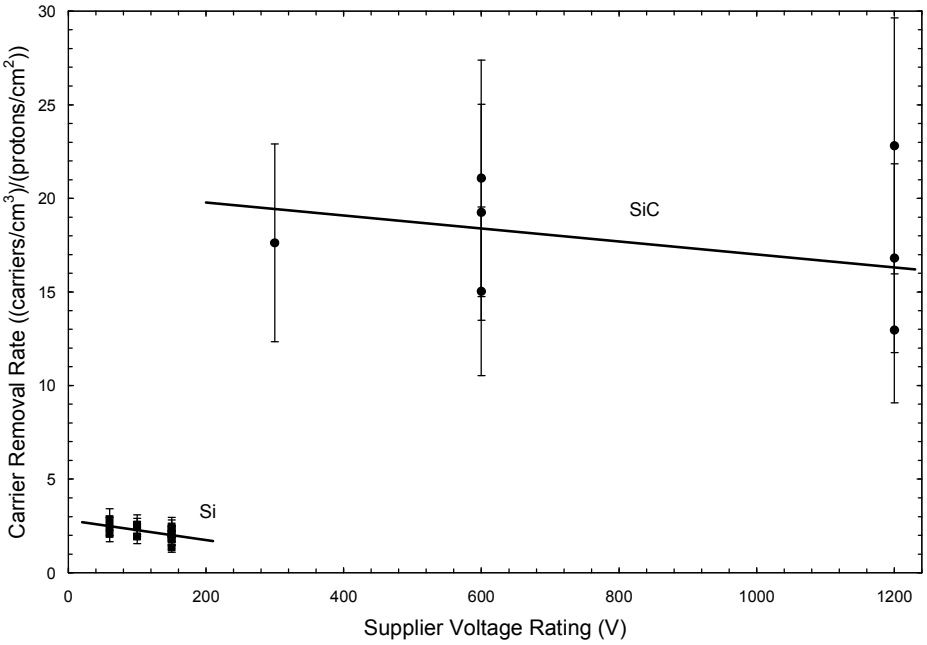

Fig. 9 Plot of carrier removal rate for SiC and Si *vs.* the supplier voltage rating for the Schottky diodes. The lines are merely meant to guide the eye.

The conventional wisdom that SiC should be the harder material appears to come from two origins. First is the "apples and oranges" comparison of looking at just Si p-n diodes and SiC Schottky diodes. As can be seen from Fig. 3, this comparison would lead to the conclusion that SiC was more radiation tolerant. No previous literature comparisons have been located that compare either p-n diodes of the different materials or Schottky diodes of the different materials. By comparing diodes made with different materials but the same type of diode, as has been done in this study, it is possible to remove the fundamental p-n *vs.* Schottky difference from the analysis.

Second, is the well established consideration that displacement energies, for both species, in SiC are larger than in Si [8]. The lower displacement energy in Si indicates that the primary damage process will produce more Frenkel pairs in Si, but says nothing about what happens immediately after. The present work suggests that there must be more immediate recombination of these primary pairs in SiC than in Si; i.e., the net result of initial damage production plus initial recovery is less in Si than in SiC, at least at room temperature where these studies were performed.

5.0 Conclusion

The carrier removal rates in Si and SiC have been calculated for 203 MeV proton irradiation. The resulting values are lower for Si than for SiC. This observation demonstrates that Si is more robust with respect to proton irradiation than SiC.

6.0 Recommendations for Future Work

As a continuation of this work, there are three areas that could be addressed next. The three are separate and could be pursued either together or separately.

1) The fiscal year 2007 (FY07) task focused on Schottky diodes to separate out the carrier removal rate as that is the only sensitive parameter in these majority carrier devices. Performing similar experiments on p-n diodes would permit comparison of the carrier lifetimes in these minority carrier devices.
2) There was discussion of polytype effects at 2007 IEEE Nuclear and Space Radiation Effects Conference (NSREC 2007) with evidence presented that the carrier removal rate was much lower in the 6H polytype than in 4H polytype [9]. This claim needs to be verified and also extended to include the 3C polytype. While the 4H polytype is the most common commercial material due to its superior electrical properties, the other two polytypes are routinely produced by many groups and so devices from all three are readily available.
3) The FY07 studies all dealt with room temperature effects. It would be desirable to extend these studies to other temperatures.

7.0 Acknowledgment

The author would like to thank Philip G. Neudeck of the NASA Glenn Research Center and Anant Agarwal of Cree, Inc. for helpful discussions.

8.0 REFERENCES

[1] R.D. Harris, A.J. Frasca, and M.O. Patton, "Displacement damage effects on the forward bias characteristics of SiC Schottky barrier power diodes," IEEE Trans. Nucl. Sci., vol. 52, no. 6, pp. 2408–2412, Dec. 2005.

[2] R.D. Harris, and A.J. Frasca, "Proton irradiation of silicon Schottky barrier power diodes," IEEE Trans. Nucl. Sci., vol. 53, no. 4, pp. 1995–2003, Aug. 2006.

[3] J.M. McGarrity, F.B. McLean, W.M. Delancey, J. Palmour, C. Carter, J. Edmond, and R.E. Oakley, "Silicon carbide JFET Radiation Response," IEEE Trans. Nucl. Sci., vol. 39, no. 6, pp. 1974–1981, Dec. 1992.

[4] F.B. McLean, J.M. McGarrity, and C.J. Scozzie, "Analysis of neutron damage in high-temperature silicon carbide JFETs," IEEE Trans. Nucl. Sci., vol. 41, no. 6, pp. 1884–1894, Dec. 1994.

[5] C.J. Scozzie, J.M. McGarrity, J. Blackburn, and W.M. DeLancey, "Silicon carbide FETs for high temperature nuclear environments," IEEE Trans. Nucl. Sci., vol. 43, no. 3, pp. 1642–1648, June 1996.

[6] S.M. Sze, *Physics of Semiconductor Devices*, New York: Wiley, 1969.

[7] R.D. Harris and A.J. Frasca, to be published.

[8] A.L. Barry, B. Lehmann, D. Fritsch, and D. Braunig, "Energy dependence of electron damage and displacement threshold energy in 6H silicon carbide," IEEE Trans. Nucl. Sci., vol. 38, no. 6, pp. 1111–1115, Dec. 1991.

[9] S.C. Witczak, W.A. Martin, R. Koga, J.R. Srour, S.R. Nuccio, and J.V. Osborn, "Displacement damage effects in irradiated silicon carbide devices," presented at NSREC 2007, to be published.

APPENDIX A DETAILS OF SiC C-V MEASUREMENTS

The free carrier concentration of a diode can be determined from C-V measurements. The relationship has been given above in (1). Plots of $1/C^2$ *vs. V* have been made for each part type and are depicted in the figures in these appendices.

The straight lines in the figures are fits to the data for each individual device measured. The slope is given from (1) as:

$$slope = 2/q\varepsilon\varepsilon_0 N_D A^2 , \qquad \text{(A1)}$$

from which the carrier concentration, N_D, can be calculated. The average values determined for each part type are listed in Table II.

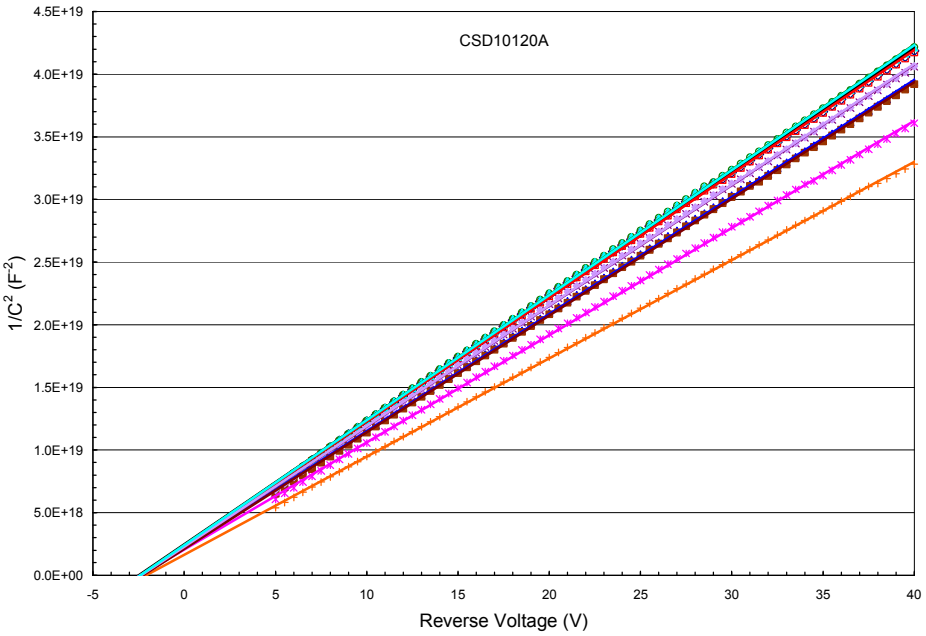

Fig. A-1 Plot of $1/C^2$ *vs. V* for SiC part CSD10120A. 10 parts are included.

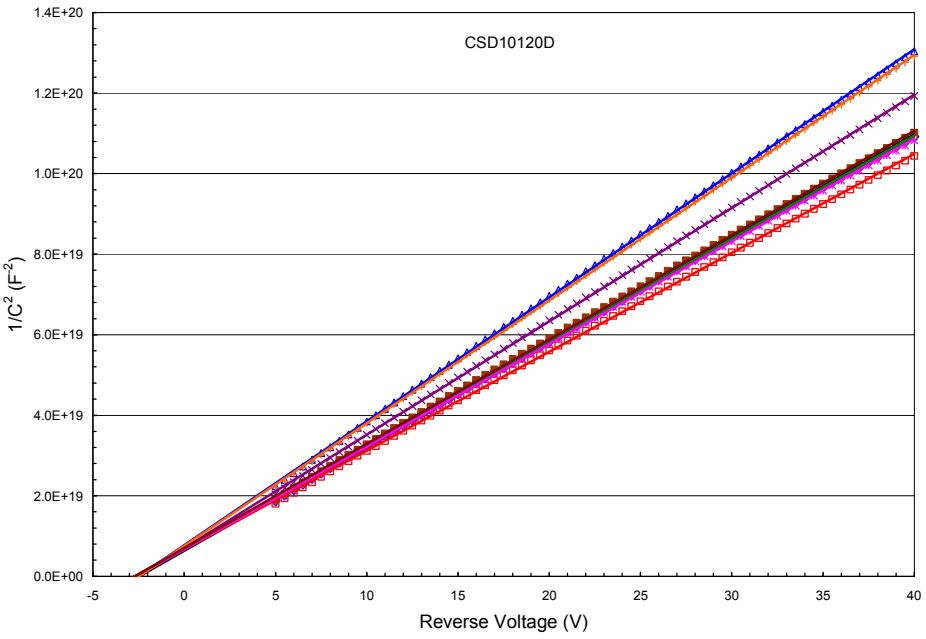

Fig. A-2 Plot of $1/C^2$ *vs. V* for SiC part CSD10120D. 8 parts are included.

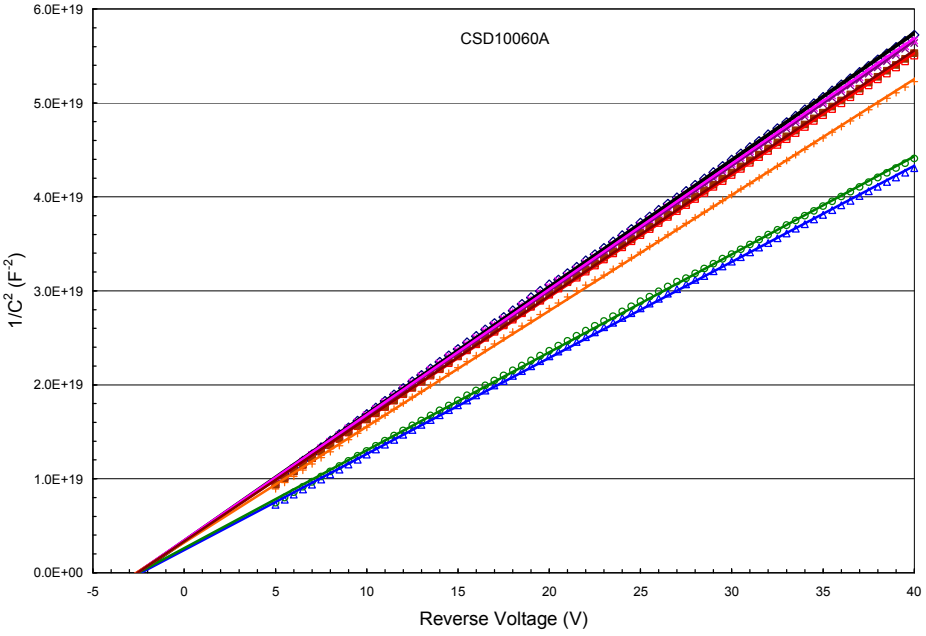

Fig. A-3 Plot of $1/C^2$ *vs. V* for SiC part CSD10060A. 8 parts are included.

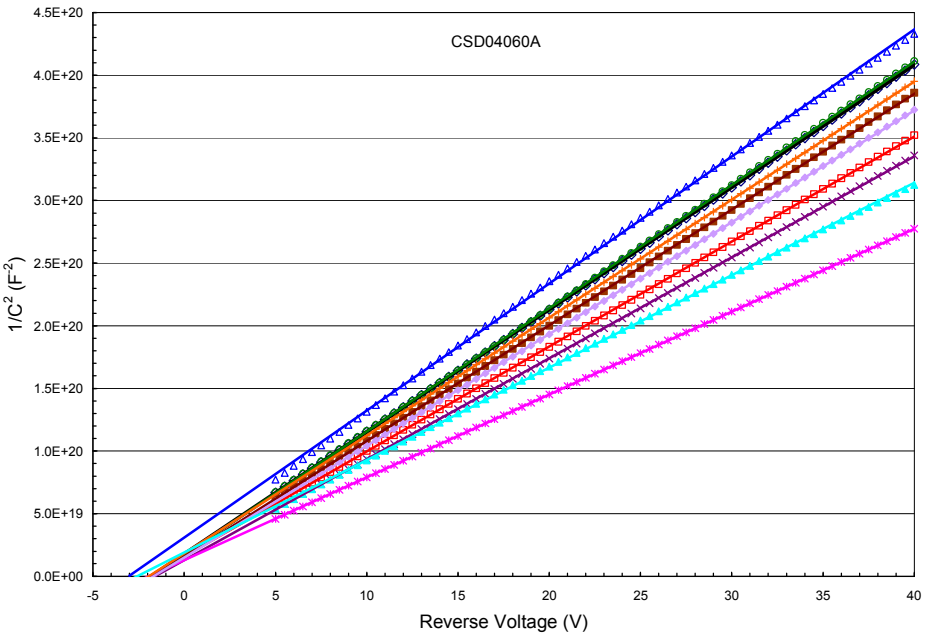

Fig. A-4 Plot of $1/C^2$ *vs. V* for SiC part CSD04060A. 10 parts are included.

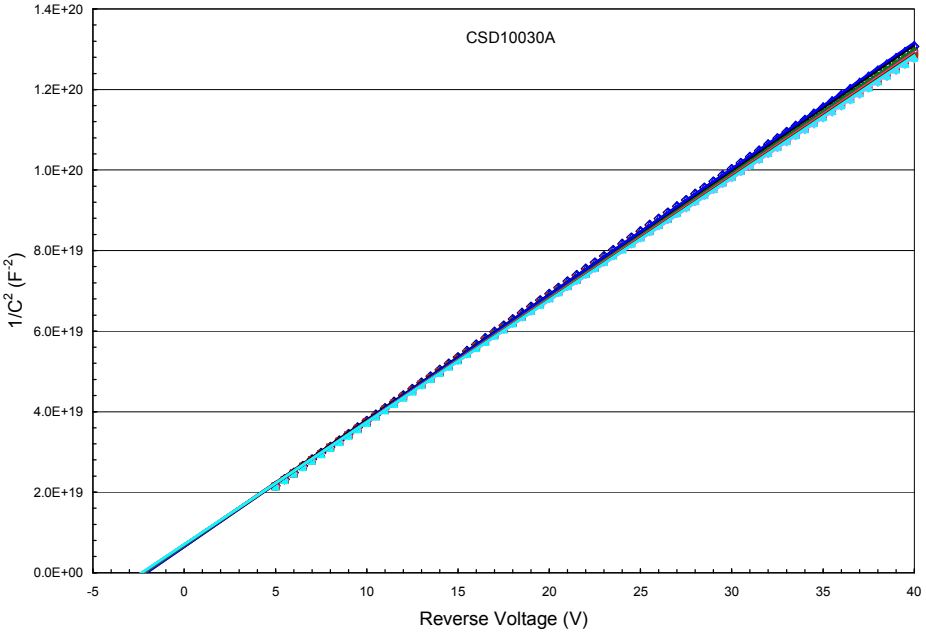

Fig. A-5 Plot of $1/C^2$ *vs. V* for SiC part CSD10030A. 10 parts are included.

APPENDIX B DETAILS OF SI C-V MEASUREMENTS

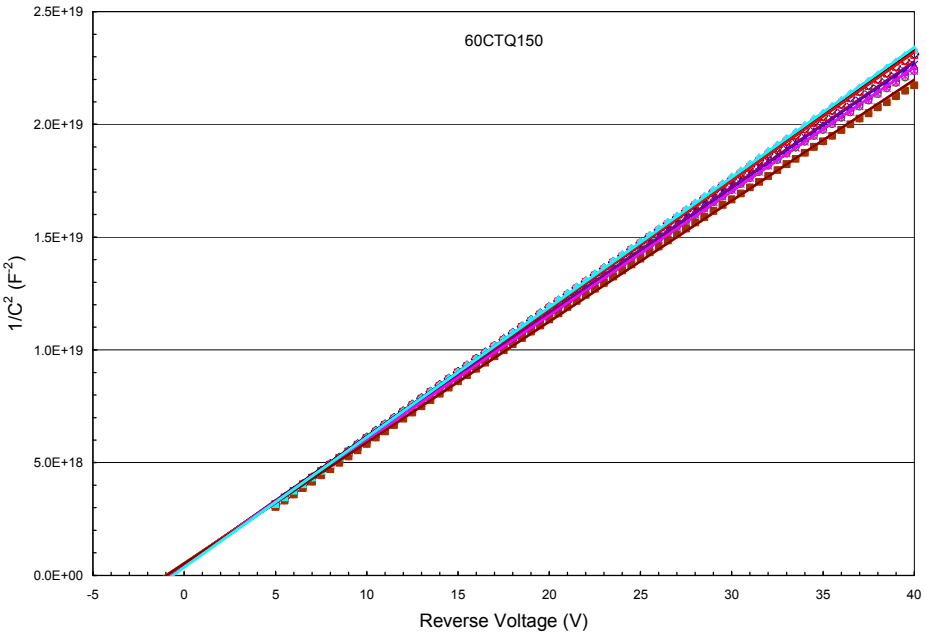

Fig. B-1 Plot of $1/C^2$ *vs.* V for Si part 60CTQ150. 10 parts are included.

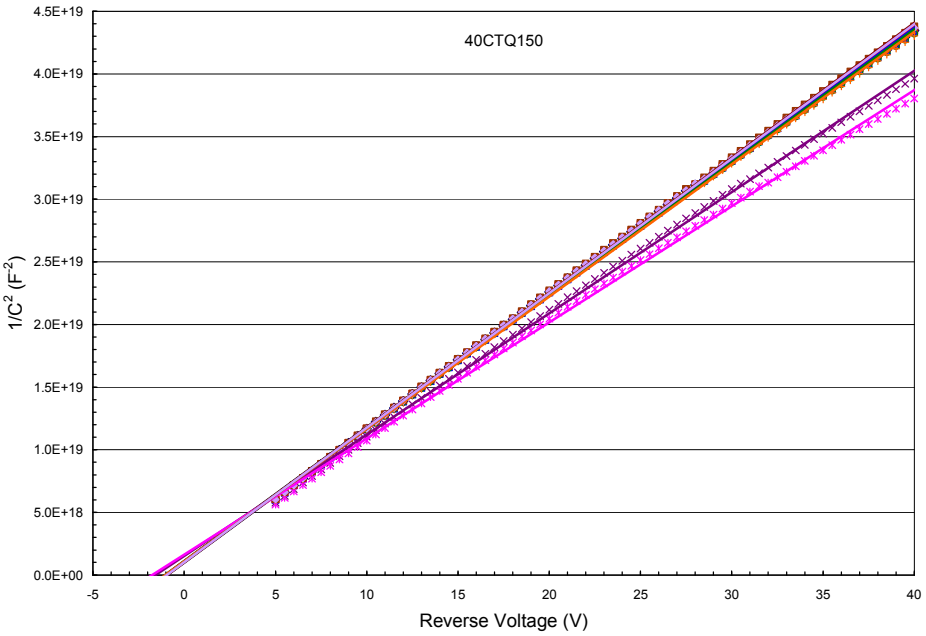

Fig. B-2 Plot of $1/C^2$ *vs.* V for Si part 40CTQ150. 9 parts are included.

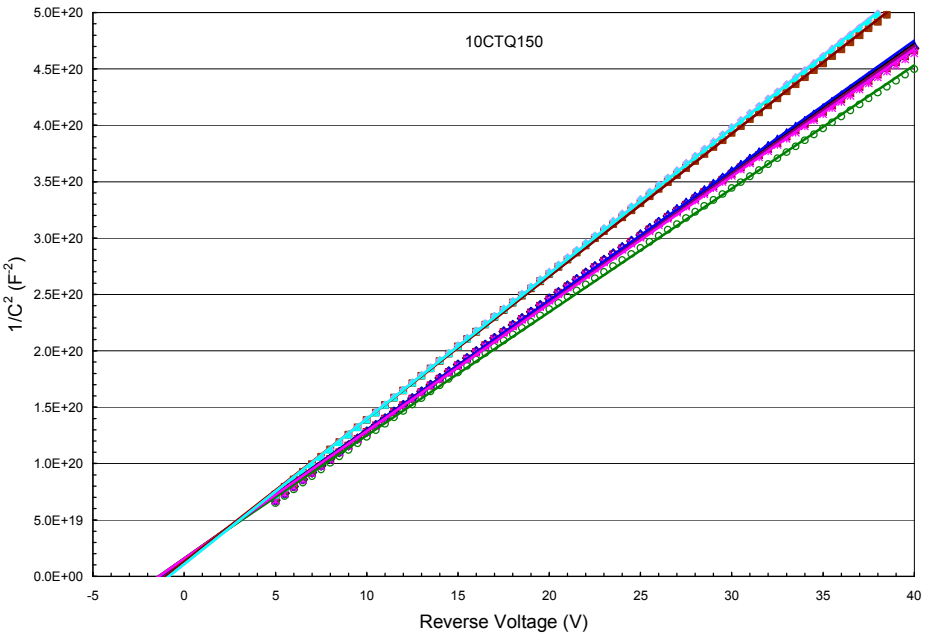

Fig. B-3 Plot of $1/C^2$ *vs. V* for Si part 10CTQ150. 10 parts are included.

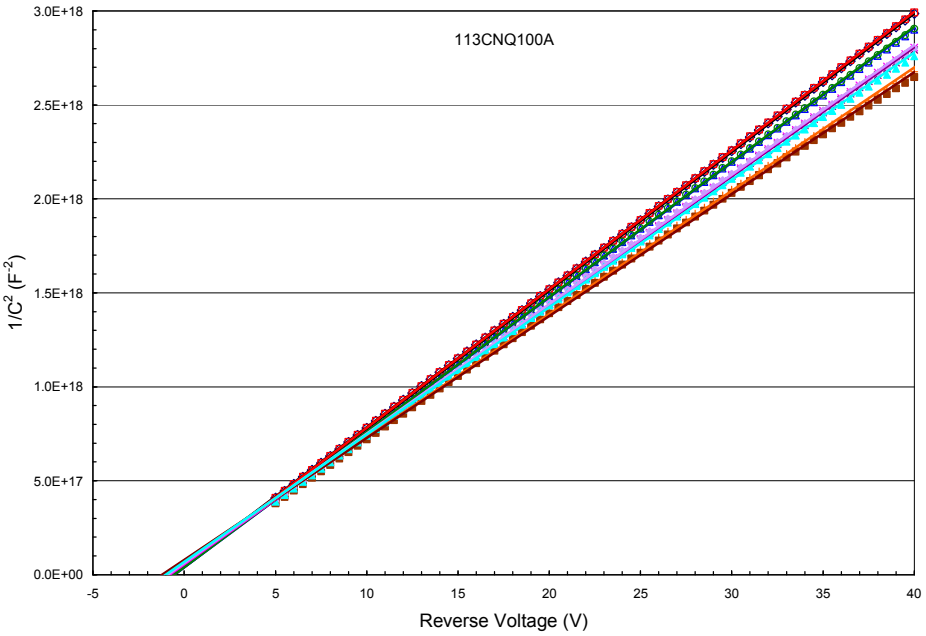

Fig. B-4 Plot of $1/C^2$ *vs. V* for Si part 113CNQ100A. 10 parts are included.

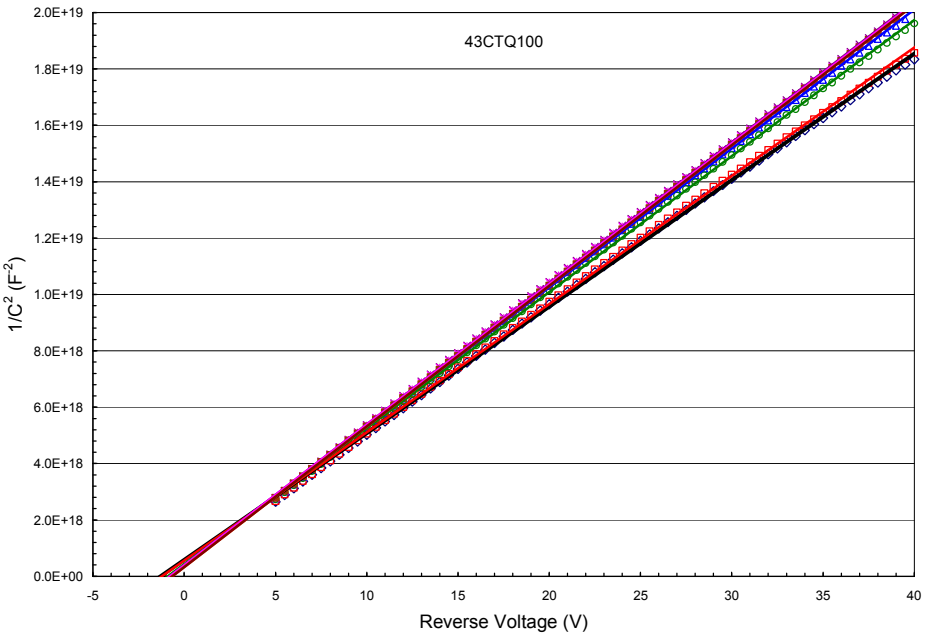

Fig. B-5 Plot of $1/C^2$ *vs. V* for Si part 43CTQ100. 8 parts are included.

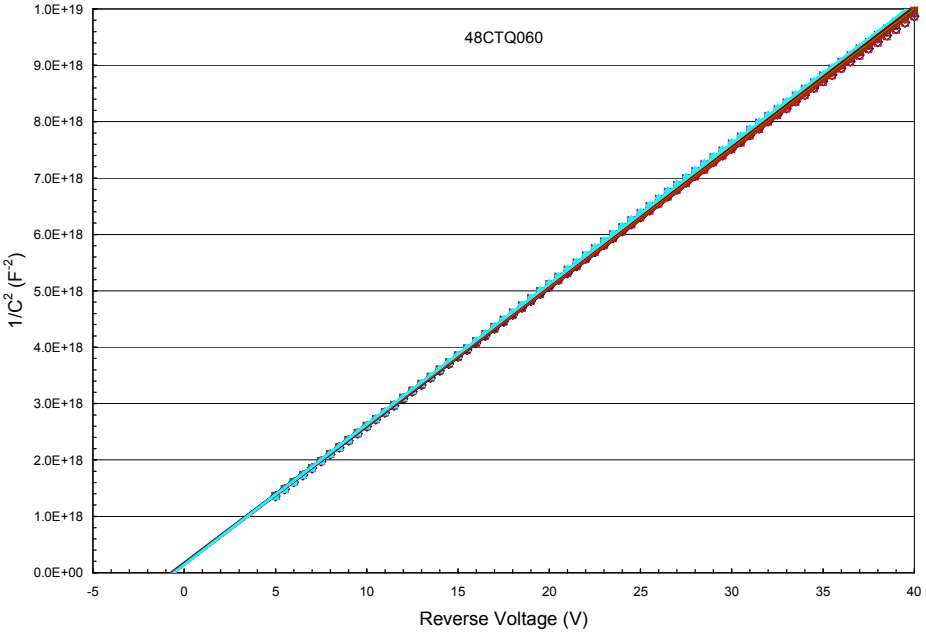

Fig. B-6 Plot of $1/C^2$ *vs. V* for Si part 48CTQ060. 10 parts are included.